Available online at www.sciencedirect.com
ScienceDirect
Journal of Sound and Vibration 314 (2008) 837–850
JOURNAL OF SOUND AND VIBRATION
www.elsevier.com/locate/jsvi

Accurate and elegant free vibration and buckling studies of orthotropic rectangular plates using untruncated infinite series

S. Kshirsagar, K. Bhaskar*

Aerospace Engineering Department, Indian Institute of Technology, Madras, Chennai 600 036, India

Received 10 May 2007; received in revised form 5 October 2007; accepted 4 January 2008
Handling Editor: L.G. Tham
Available online 15 February 2008

Abstract

This paper presents the extension of a novel superposition method, put forth for static analysis earlier, for carrying out free vibration and bifurcation buckling studies of orthotropic rectangular plates with any combination of classical boundary conditions viz. clamped, simply supported and free edges. It is shown that use of infinite series counterparts of conventional Levy-type closed-form expressions result in a tremendous simplification of the problem without any compromise on accuracy. The complicating effects of an elastic foundation and initial stresses are also shown to be easily accounted for. Results, useful as benchmarks in future, are presented for a chosen set of cases.

1. Introduction

While rectangular plates with at least two opposite edges simply supported are amenable to exact analysis, those with other boundary conditions are difficult to handle and are often analysed approximately using the direct methods of variational calculus. However, it has been shown [1] that superposition of appropriate Levy-type solutions provides a powerful approach for such problems since the governing differential equation is satisfied rigorously at every stage and the boundary conditions can be satisfied in a series sense to any desired degree of accuracy; the methodology has to be termed exact since the convergence of the Fourier series employed for edge forces/moments in the different building blocks is guaranteed. The only disadvantage with this approach is the need to derive the Levy-type solutions for each building block, which are not only lengthy and tedious, but also of different forms depending on the nature of the characteristic roots of the associated ordinary differential equation; further, the hyperbolic functions employed in the Levy-type solutions give rise to numerical difficulties when their arguments are large. Both these difficulties prove to be serious handicaps when the material is anisotropic or when the problem is governed by a high-order system of governing equations, which arise when one tries to account for bending–stretching coupling or non-classical shear deformation effects. The aforementioned difficulties have been elaborately discussed earlier and alternative approximate building block solutions have been suggested as a way out [2,3].

*Corresponding author. Tel.: +91 44 22574010; fax: +91 44 22574002.
E-mail address: kbhas@ae.iitm.ac.in (K. Bhaskar).

0022-460X/$ - see front matter © 2008 Elsevier Ltd. All rights reserved.
doi:10.1016/j.jsv.2008.01.013

In this context, a novel superposition approach has been expounded recently for problems of static flexure [4,5], the distinguishing feature being the use of untruncated series counterparts of the conventional lengthy Levy-type expressions without any loss of rigour or accuracy. These counterpart solutions are easy to derive, are of the same form irrespective of the nature of the roots of the characteristic equation, and lead to no further numerical difficulties. The ease and utility of this method, referred to as *Untruncated Infinite Series Superposition Method* (UISSM), have also been illustrated for unsymmetric laminates [6,7] and for shear-deformable plates [8,9]. The objective of this paper is to extend this method for free vibration and buckling studies and to demonstrate its superiority with respect to conventional analysis, with attention confined to thin homogeneous specially orthotropic plates or symmetric cross-ply plates with the complicating effects of initial stresses and an elastic foundation.

2. Methodology

2.1. Plates with clamped/simply supported edges

The problem of the rectangular plate ($0 \leqslant x, y \leqslant a, b$) with any combination of simply supported and clamped edges is looked upon as that of superposition of some or all of the building blocks shown in Fig. 1, each of them with only simply supported edges; the edge moments are assumed, without loss of generality, to be of the form

$$(M_{\text{top}}, M_{\text{bottom}}) = \sum_m (M_{tm}, M_{bm}) \sin\left(\frac{m\pi x}{a}\right) e^{i\omega t},$$
$$(M_{\text{left}}, M_{\text{right}}) = \sum_n (M_{ln}, M_{rn}) \sin\left(\frac{n\pi y}{b}\right) e^{i\omega t}. \quad (1)$$

If the problem involves an elastic foundation and/or initial stresses due to uniform edge forces N_x, N_y (taken to be positive when tensile), they are applicable to each building block. The plate is assumed to be orthotropic with the principal material directions coinciding with the x and y axes, and has a mass per unit area ρ. The foundation is of the Winkler type with stiffness k_F.

Considering the conventional Levy-type solution first, let us focus attention on the second building block. The governing equation of the classical plate theory is

$$D_{11}w_{,xxxx} + 2(D_{12} + 2D_{66})w_{,xxyy} + D_{22}w_{,yyyy} + k_F w + \rho w_{,tt} = N_x w_{,xx} + N_y w_{,yy}, \quad (2)$$

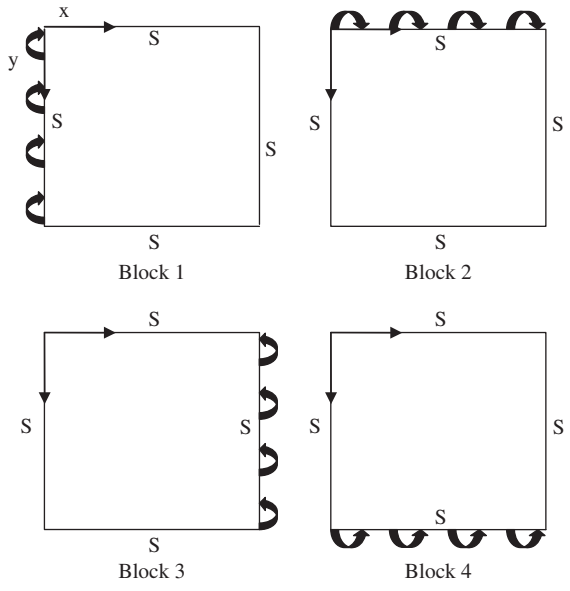

Fig. 1. Building blocks for clamped/simply supported plates.

where a subscript comma denotes differentiation, and the D_{ij}'s are the bending stiffness coefficients occurring in the moment curvature relations

$$\begin{Bmatrix} M_x \\ M_y \\ M_{xy} \end{Bmatrix} = \begin{bmatrix} D_{11} & D_{12} & 0 \\ & D_{22} & 0 \\ \text{sym.} & & D_{66} \end{bmatrix} \begin{Bmatrix} -w_{,xx} \\ -w_{,yy} \\ -2w_{,xy} \end{Bmatrix}. \tag{3}$$

The Levy-type solution is sought as

$$w = \sum_m W_m(y) \sin\left(\frac{m\pi x}{a}\right) e^{i\omega t}, \tag{4}$$

which identically satisfies the simple support conditions at $x = 0, a$. One can immediately see that the governing equation is reduced to a fourth-order ordinary differential equation in W_m, and enforcement of boundary conditions at the top and bottom edges yields W_m. However, the general solution of the fourth-order equation is of different forms depending on the nature of roots of the characteristic equation, which in turn depend on the frequency ω and the in-plane loads. These different forms have been discussed earlier with reference to isotropic [10] and orthotropic plates [11] without any complicating effects, and are as presented in Table 1.

Thus, even for the simplest case of the isotropic plate without any complicating effects, there exist two solutions for building block 2, as given by

$$W_m = \frac{M_{tm}}{2\omega\sqrt{\rho D}} \Big[-\cos\sqrt{k^2-\alpha^2}y + \cosh\sqrt{k^2+\alpha^2}y + \cot\sqrt{k^2-\alpha^2}b \sin\sqrt{k^2-\alpha^2}y - \coth\sqrt{k^2+\alpha^2}b \sinh\sqrt{k^2+\alpha^2}y \Big] \quad \text{for } k^2 > \alpha^2, \tag{5a}$$

$$\frac{M_{tm}}{2\omega\sqrt{\rho D}} \Big[-\cosh\sqrt{\alpha^2-k^2}y + \cosh\sqrt{k^2+\alpha^2}y + \coth\sqrt{\alpha^2-k^2}b \sinh\sqrt{\alpha^2-k^2}y - \coth\sqrt{k^2+\alpha^2}b \sinh\sqrt{k^2+\alpha^2}y \Big] \quad \text{for } k^2 < \alpha^2, \tag{5b}$$

where $k^4 = \rho\omega^2/D$, $\alpha = m\pi/a$. Such alternative solution forms would exist for each building block and all such possible forms need to be explicitly written down before the appropriate ones are superposed.

The above difficulty becomes very serious when one or more complicating effects are accounted for. For example, it has been pointed out [10] that the presence of in-plane forces would necessitate the consideration of a greater number of solution forms even for a thin isotropic plate than those shown in Table 1. Further, when unsymmetric lay-ups or shear deformation effects are considered, the order of the system of governing equations increases and so does the number of possible solution forms associated with various root combinations. This difficulty has been pointed out as the major handicap, besides the possibility of numerical errors due to hyperbolic functions with large arguments, when the conventional superposition method is employed for complicated plate problems [2,3].

All the aforementioned disadvantages are overcome in the UISSM employed here; the basic idea is to seek a solution not in the form of a single series as in Eq. (3), but in the form of a double series. For the second building block, it is sought as

$$w = \sum_m \sum_{n=1}^{\infty} W_{mn} \sin\left(\frac{n\pi y}{b}\right) \sin\left(\frac{m\pi x}{a}\right) e^{i\omega t}. \tag{6}$$

Corresponding to any particular harmonic M_{tm} of the applied moment, the deflection function is obtained using the principle of virtual work as given by

$$\iint (-M_x \delta w_{,xx} - M_y \delta w_{,yy} - 2M_{xy}\delta w_{,xy})\,dx\,dy = \int_{x=0}^{a} M_{tm} \sin\frac{m\pi x}{a} e^{i\omega t} (\delta w_{,y})\big|_{y=0}\,dx - \iint (\rho w_{,tt}\delta w)\,dx\,dy - \iint (N_x w_{,x}\delta w_{,x})\,dx\,dy - \iint (N_y w_{,y}\delta w_{,y})\,dx\,dy - \iint (k_F w \delta w)\,dx\,dy. \tag{7}$$

Table 1
Different forms for $W_m(y)$ in the conventional Levy-type solution

Case	W_m
Isotropic	
(1) For $\left(\frac{m\pi}{a}\right)^2 < \left(\frac{\rho\omega^2}{D}\right)^{1/2}$	$W_m = A_m \sinh(\lambda_2 y) + B_m \cosh(\lambda_2 y) + C_m \sin(\lambda_1 y) + D_m \cos(\lambda_1 y)$ where $\lambda_1 = \left[\left(\frac{\rho\omega^2}{D}\right)^{1/2} - \left(\frac{m\pi}{a}\right)^2\right]^{1/2}$, $\lambda_2 = \left[\left(\frac{\rho\omega^2}{D}\right)^{1/2} + \left(\frac{m\pi}{a}\right)^2\right]^{1/2}$
(2) For $\left(\frac{m\pi}{a}\right)^2 > \left(\frac{\rho\omega^2}{D}\right)^{1/2}$	$W_m = A_m \sinh(\lambda_2 y) + B_m \cosh(\lambda_2 y) + C_m \sinh(\lambda_1 y) + D_m \cosh(\lambda_1 y)$ where $\lambda_1 = \left[\left(\frac{m\pi}{a}\right)^2 - \left(\frac{\rho\omega^2}{D}\right)^{1/2}\right]^{1/2}$, $\lambda_2 = \left[\left(\frac{m\pi}{a}\right)^2 + \left(\frac{\rho\omega^2}{D}\right)^{1/2}\right]^{1/2}$
Orthotropic	
(1) For $\left[\left(\frac{D_{12}+2D_{66}}{D_{22}}\right)^2 - \frac{D_{11}}{D_{22}} + \left(\frac{\rho\omega^2}{\alpha^4 D_{22}}\right)\right] > 0$ and $\left[\left(\frac{D_{12}+2D_{66}}{D_{22}}\right)^2 - \frac{D_{11}}{D_{22}} + \left(\frac{\rho\omega^2}{\alpha^4 D_{22}}\right)\right]^{1/2} > \frac{(D_{12}+2D_{66})}{D_{22}}$ where $\alpha = \left(\frac{m\pi}{a}\right)$	$W_m = A_m \sinh(\phi y) + B_m \cosh(\phi y) + C_m \sin(\psi y) + D_m \cos(\psi y)$ $\phi = \alpha\left\{\left[\left(\frac{D_{12}+2D_{66}}{D_{22}}\right)^2 - \frac{D_{11}}{D_{22}} + \left(\frac{\rho\omega^2}{\alpha^4 D_{22}}\right)\right]^{1/2} + \frac{(D_{12}+2D_{66})}{D_{22}}\right\}^{1/2}$ $\psi = \alpha\left\{\left[\left(\frac{D_{12}+2D_{66}}{D_{22}}\right)^2 - \frac{D_{11}}{D_{22}} + \left(\frac{\rho\omega^2}{\alpha^4 D_{22}}\right)\right]^{1/2} - \frac{(D_{12}+2D_{66})}{D_{22}}\right\}^{1/2}$
(2) For $\left[\left(\frac{D_{12}+2D_{66}}{D_{22}}\right)^2 - \frac{D_{11}}{D_{22}} + \left(\frac{\rho\omega^2}{\alpha^4 D_{22}}\right)\right] > 0$ and $\left[\left(\frac{D_{12}+2D_{66}}{D_{22}}\right)^2 - \frac{D_{11}}{D_{22}} + \left(\frac{\rho\omega^2}{\alpha^4 D_{22}}\right)\right]^{1/2} < \frac{(D_{12}+2D_{66})}{D_{22}}$	$W_m = A_m \sinh(\phi y) + B_m \cosh(\phi y) + C_m \sinh(\psi y) + D_m \cosh(\psi y)$ $\phi = \alpha\left\{\left[\left(\frac{D_{12}+2D_{66}}{D_{22}}\right)^2 - \frac{D_{11}}{D_{22}} + \left(\frac{\rho\omega^2}{\alpha^4 D_{22}}\right)\right]^{1/2} + \left(\frac{D_{12}+2D_{66}}{D_{22}}\right)\right\}^{1/2}$ $\psi = \alpha\left\{\left(\frac{D_{12}+2D_{66}}{D_{22}}\right) - \left[\left(\frac{D_{12}+2D_{66}}{D_{22}}\right)^2 - \frac{D_{11}}{D_{22}} + \left(\frac{\rho\omega^2}{\alpha^4 D_{22}}\right)\right]^{1/2}\right\}^{1/2}$
(3) For $\left[\left(\frac{D_{12}+2D_{66}}{D_{22}}\right)^2 - \frac{D_{11}}{D_{22}} + \left(\frac{\rho\omega^2}{\alpha^4 D_{22}}\right)\right] < 0$	$W_m = A_m \sin(\theta_2 y)\sinh(\theta_1 y) + B_m \sin(\theta_2 y)\cosh(\theta_1 y) + C_m \cos(\theta_2 y)\sinh(\theta_1 y) + D_m \cos(\theta_2 y)\cosh(\theta_1 y)$ where $\theta_1 = \alpha\sqrt[4]{c^2+d^2}\cos\left[\frac{\tan^{-1}(c/d)}{2}\right]$, $\theta_2 = \alpha\sqrt[4]{c^2+d^2}\sin\left[\frac{\tan^{-1}(c/d)}{2}\right]$ $c = \left[\left(\frac{D_{12}+2D_{66}}{D_{22}}\right)^2 - \frac{D_{11}}{D_{22}} + \left(\frac{\rho\omega^2}{\alpha^4 D_{22}}\right)\right]^{1/2}$; $d = \frac{(D_{12}+2D_{66})}{D_{22}}$

Substitution for w from Eq. (6) and use of the orthogonality relations of the trigonometric functions given by

$$\int_{s=0}^{l} \sin\frac{\alpha\pi s}{l}\sin\frac{\beta\pi s}{l}\,\mathrm{d}s = \int_{s=0}^{l} \cos\frac{\alpha\pi s}{l}\cos\frac{\beta\pi s}{l}\,\mathrm{d}s = l/2 \text{ for } \alpha=\beta, 0 \text{ for } \alpha\neq\beta \tag{8}$$

yields W_{mn} as

$$W_{mn} = \frac{2M_{tm}n\pi}{b^2\Gamma(a,b)}, \tag{9}$$

where the function $\Gamma(a,b)$ is given by

$$\Gamma(a,b) = D_{11}\left(\frac{m\pi}{a}\right)^4 + 2(D_{12}+D_{66})\left(\frac{m\pi}{a}\right)^2\left(\frac{n\pi}{b}\right)^2 + D_{22}\left(\frac{n\pi}{b}\right)^4 + k_F - \rho\omega^2 + N_x\left(\frac{m\pi}{a}\right)^2 + N_y\left(\frac{n\pi}{b}\right)^2. \tag{10}$$

Thus, the solution for the second building block is now given by

$$w = \sum_m M_{tm} \sin\frac{m\pi x}{a} e^{i\omega t} \sum_{n=1}^{\infty} \frac{2n\pi}{b^2\Gamma(a,b)} \sin\frac{n\pi y}{b} \tag{11}$$

with the untruncated infinite series (with index n) replacing the closed-form $W_m(y)$ of the type shown in Eqs. (5a) and (5b).

It can be proved that there is no approximation involved in the above methodology and that the series solution is also an exact solution. This can be done by expanding *either* of the closed-form expressions of Eq. (5a) or (5b) in a half-range sine series in the interval $(0,b)$; the resulting Fourier coefficients are

$$\frac{2M_{tm}n\pi}{b^2 D\left\{\left[(m\pi/a)^2 + (n\pi/b)^2\right]^2 - \rho\omega^2/D\right\}}. \tag{12}$$

These can be seen to be identical as those of Eq. (9) when specialized for this isotropic case.

Thus, the use of the principle of virtual work generates an exact series counterpart of the Levy-type solution and this series counterpart is unique in the sense it can be used in place of all the different closed-form expressions that need to be explicitly written down for various root combinations in the conventional superposition approach. This advantage cannot be overemphasized because, as mentioned earlier, the number of possible root combinations is quite large for complicated plate problems, and further, each of the different closed-form expressions is often quite tedious and lengthy; the new approach completely obviates the need to identify the different root combinations and the derivation of the tedious Levy-type expressions.

The exact series solutions for the other building blocks of Fig. 1 are obtained in the same manner as above; the solution for the fourth building block is also of the form of Eq. (6), while for the first and the third, the solutions are of the form

$$w = \sum_n \sum_{m=1}^{\infty} W_{mn} \sin\left(\frac{m\pi x}{a}\right) \sin\left(\frac{n\pi y}{b}\right) e^{i\omega t}. \tag{13}$$

The corresponding W_{mn} is given by

$$W_{mn} = \frac{-2M_{rn}m\pi\cos m\pi}{a^2\Gamma(a,b)} \text{ or } \frac{-2M_{bm}n\pi\cos n\pi}{b^2\Gamma(a,b)} \text{ or } \frac{2M_{ln}m\pi}{a^2\Gamma(a,b)} \tag{14}$$

as the case may be.

The final step involves superposition of the appropriate building blocks based on the number of clamped edges (block 1 if the left edge is clamped, and so on) and setting up the eigenvalue problem by writing down the zero slope condition at each clamped edge. To illustrate this, plates with two opposite simply supported edges ($x = 0$, a) are considered first; the conventional Levy-type solution for such plates leads to complete uncoupling of the different harmonics (m) in the x-direction and yields a transcendental equation, similar to that for one-dimensional problems, for each m. For plates without in-plane forces or the elastic foundation, such frequency equations are as presented in Table 2 where the different alternative solution forms of Table 1 are duly considered. The plates are designated as SCSS, etc. where S denotes a simply supported edge, C a clamped edge and the boundary conditions are specified in a clockwise sense starting from the left edge $x = 0$. When these plates are analyzed using the untruncated infinite series approach, the SCSS plate requires building block 2 alone while the SCSC plate requires building blocks 2 and 4. The zero slope conditions (at the top edge, or top and bottom edges as the case may be) yield homogeneous equations in terms of the moment coefficients (M_{tm} or M_{tm} and M_{bm}) and the frequency equation is obtained by seeking a non-trivial solution for these unknowns; since the coefficients occurring in these homogeneous equations are untruncated infinite sums

Table 2
Different forms of the frequency equation for the cases of Table 1

Material	Edge conditions	Frequency equation
Isotropic	SCSS	Case 1: $\lambda_1 \sinh(\lambda_2 b)\cos(\lambda_1 b) - \lambda_2 \cosh(\lambda_2 b)\sin(\lambda_1 b) = 0$[a] Case 2: $\lambda_1 \sinh(\lambda_2 b)\cosh(\lambda_1 b) - \lambda_2 \cosh(\lambda_2 b)\sinh(\lambda_1 b) = 0$
Isotropic	SCSC	Case 1: $2\lambda_1\lambda_2[\cos(\lambda_1 b)\cosh(\lambda_2 b) - 1] + (\lambda_1^2 - \lambda_2^2)\sinh(\lambda_2 b)\sin(\lambda_1 b) = 0$ Case 2: $2\lambda_1\lambda_2[\cosh(\lambda_1 b)\cosh(\lambda_2 b) - 1] - (\lambda_1^2 + \lambda_2^2)\sinh(\lambda_2 b)\sinh(\lambda_1 b) = 0$
Orthotropic	SCSS	Case 1: $\psi \sinh(\phi b)\cos(\psi b) - \phi \cosh(\phi b)\sin(\psi b) = 0$ Case 2: $\psi \sinh(\phi b)\cosh(\psi b) - \phi \cosh(\phi b)\sinh(\psi b) = 0$ Case 3: $\sin(2\theta_2 b)\theta_1 - \sinh(2\theta_1 b)\theta_2 = 0$
Orthotropic	SCSC	Case 1: $\alpha^2\left(\frac{D_{12}+2D_{66}}{D_{22}}\right)\sinh(\phi b)\sin(\psi b) + \phi\psi[1 - \cosh(\phi b)\cos(\psi b)] = 0$ Case 2: $\alpha^2\left(\frac{D_{12}+2D_{66}}{D_{22}}\right)\sinh(\phi b)\sinh(\psi b) + \phi\psi[1 - \cosh(\phi b)\cosh(\psi b)] = 0$ Case 3: $\theta_1^2 \sin^2(\theta_2 b) - \theta_2^2 \sinh^2(\theta_1 b) = 0$

[a]All parameters as defined in Table 1 for the appropriate case.

Table 3
Frequency equations of UISSM applicable for isotropic/orthotropic plates over the entire frequency range

Plate	Frequency equation
SCSS	$\sum_{n=1}^{\infty} \frac{(n\pi)^2}{\Gamma(a,b)} = 0$
SCSC	$\text{Det}\begin{vmatrix} \sum_{n=1}^{\infty} \frac{(n\pi)^2}{\Gamma(a,b)} & \sum_{n=1}^{\infty} \frac{(n\pi)^2 \cos n\pi}{\Gamma(a,b)} \\ \sum_{n=1}^{\infty} \frac{(n\pi)^2 \cos n\pi}{\Gamma(a,b)} & \sum_{n=1}^{\infty} \frac{(n\pi)^2}{\Gamma(a,b)} \end{vmatrix} = 0$

Note: Γ is defined in Eq. (10).

(see Eq. (6)), the frequency equation is also in terms of untruncated infinite sums, as given in Table 3. Such a frequency equation is now unique over the entire frequency range and is the counterpart of all the different variants of Table 2; further, the incorporation of the complicating effects of in-plane forces or an elastic foundation in this series approach requires no procedural changes or complexities, but only that such terms be considered in the definition of Γ (Eq. (10)).

To illustrate the application of UISSM for plates without two opposite edges simply supported, let us consider the doubly symmetric modes of a clamped plate, for which all the four building blocks of Fig. 1 are required. However, the fixed edge moments are the same at top and bottom edges and at left and right edges, and terms with even m or n vanish in all the equations. The net deflection is given by

$$w(x,y,t) = \sum_{m=1,3,\ldots} \frac{2M_{tm}}{b^2 D} \sin\left(\frac{m\pi x}{a}\right) \sum_{n=1,3,\ldots}^{\infty} \frac{2n\pi}{\Gamma(a,b)} \sin\left(\frac{n\pi y}{b}\right) e^{i\omega t} + \sum_{n=1,3,\ldots} \frac{2M_{ln}}{a^2 D} \sin\left(\frac{n\pi y}{b}\right) \sum_{m=1,3,\ldots}^{\infty} \frac{2m\pi}{\Gamma(a,b)} \sin\left(\frac{m\pi x}{a}\right) e^{i\omega t}. \quad (15)$$

The zero slope conditions at the edges $x = 0$ and $y = 0$ yield

$$\sum_{m=1,3}^{m_{\max}} \frac{M_{tm} mn}{b^2 \Gamma(a,b)} + \frac{M_{ln}}{a^2} \sum_{m=1,3}^{\infty} \frac{m^2}{\Gamma(a,b)} = 0 \text{ for each of } n = 1, 3, \ldots, n_{\max}, \quad (16a)$$

$$\frac{M_{tm}}{b^2}\sum_{n=1,3,\ldots}^{\infty}\frac{n^2}{\Gamma(a,b)}+\sum_{n=1,3,\ldots}^{n_{\max}}\frac{M_{ln}mn}{a^2\Gamma(a,b)}=0 \text{ for each of } m=1,3,\ldots,m_{\max}, \tag{16b}$$

where $m_{\max}$ and $n_{\max}$ are the upper limits at which the moment series are truncated (see Eq. (1)). Thus, some elements of the characteristic determinant are infinite sums; it is very important to note that these infinite sums are the counterparts of the derivatives of the closed-form Levy-type expressions of the type shown in Eqs. (5a) and (5b) and have to be evaluated without truncation in order to avoid any loss of accuracy. The number of unknown moment coefficients M_{tm} and M_{ln} is chosen, as in the conventional superposition method, so as to obtain the desired convergence of the natural frequencies or buckling loads.

2.2. Plates with free edges

The building blocks required in UISSM for plates with free edges depend on the number of free edges. The methodology is explained with respect to the simple case of SSSF plate with the building blocks as shown in Fig. 2. As can be seen, they correspond to a plate either simply supported all around or with one guided edge (i.e. one that is free to translate but with the normal slope completely restrained), and subjected to edge moment or edge shear force expressed without loss of generality in the following form:

$$\text{Block 1}: M_{\text{bottom}}=\sum_m M_{bm}\sin\left(\frac{m\pi x}{a}\right)e^{i\omega t},$$
$$\text{Block 2}: V_{\text{bottom}}=\sum_m V_{bm}\sin\left(\frac{m\pi x}{a}\right)e^{i\omega t}. \tag{17}$$

The building block with the edge moment can be analyzed as discussed earlier. For block 2, the deflection function is assumed as

$$w=\sum_m\sum_{n=1}^{\infty}W_{mn}\sin\left(\frac{m\pi x}{a}\right)\sin\left(\frac{n\pi y}{2b}\right)e^{i\omega t} \tag{18}$$

and W_{mn} is obtained by employing the principle of virtual work as

$$\iint(-M_x\delta w_{,xx}-M_y\delta w_{,yy}-2M_{xy}\delta w_{,xy})\,dx\,dy=\int_{x=0}^{a}V_b\sin\frac{m\pi x}{a}e^{i\omega t}(\delta w)\big|_{y=b}\,dx$$
$$-\iint(\rho w_{,tt}\delta w)\,dx\,dy-\iint(N_x w_{,x}\delta w_{,x})\,dx\,dy-\iint(N_y w_{,y}\delta w_{,y})dx\,dy-\iint(k_F w\delta w)\,dx\,dy, \tag{19}$$

which yields

$$W_{mn}=\frac{2V_{bm}\sin(n\pi/2)}{b\Gamma(a,2b)}. \tag{20}$$

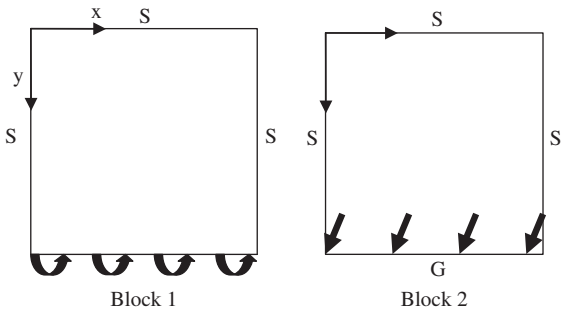

Fig. 2. Building blocks for the SSSF plate.

To determine the unknowns M_{bm} and V_{bm}, one has to impose the free edge conditions

$$M_y = 0,\ V_y - N_y w_{,y} = Q_y + M_{xy,x} - N_y w_{,y} = M_{y,y} + 2M_{xy,x} - N_y w_{,y} = 0 \quad \text{at } y = b, \tag{21}$$

where the contributions from each building block are to be calculated using the corresponding infinite series solution for w along with the moment–curvature relations, while the edge loads M_{bottom} and V_{bottom} are taken directly for the first and second building blocks, respectively. At this stage, it is very important to note that the double sine series solution (Eq. (6)) for the first building block does not yield the correct non-zero value for $w_{,yy}$ at the loaded edge $y = b$ because a simple differentiation of the series gives a zero value at this edge; thus, the series cannot be further differentiated term by term to obtain $w_{,yyy}$ which occurs in the expression for V_y; this difficulty is overcome by using Stokes' transformation [12] as explained in the Appendix.

Plates with more than one free edge can be analysed in a similar manner as above, with additional appropriately chosen building blocks as explained earlier [5] with reference to static flexure.

3. Numerical results and discussion

The main aim of the present work is to present a more convenient but equally accurate alternative to the conventional superposition method and from this viewpoint, the validation of the new approach is of primary concern. Of fundamental importance in ensuring the accuracy of UISSM is the evaluation of the infinite sums without truncation—this is possible by the use of mathematical packages like *MATLAB* or *MATHEMATICA* wherein the upper limit of summation is specified as *Infinity* and the evaluation is done by decomposing the summand into simpler partial fractions and expressing their infinite sums in terms of special functions like the gamma function.

All calculations for the present work have been carried out using *MATHEMATICA*; the accuracy of the infinite summation is first verified by comparison of the exact solutions based on the closed-form Levy-type frequency equations (Table 2) and the infinite series counterparts (Table 3) for SCSS and SCSC isotropic plates. This comparison is shown in Table 4 for square plates; the table also includes the frequencies obtained by using the equations of Table 3 with truncated summation, i.e. with the upper limit of summation taken as a finite number. From these results, it is clear that the infinite sum command of *MATHEMATICA* does ensure correct replication of the exact frequencies without any error, and further that one can also employ conventional summation with a large number of terms to obtain fairly accurate results. (It is appropriate to point out here that untruncated infinite summation takes much less time than truncated summation with a large number of terms when both are tried out using *MATHEMATICA*, presumably because the latter requires actual summation while the former is like using a look-up table of special functions. It should also be noted that the roots of the closed-form frequency equations as presented in Table 4 differ slightly—starting

Table 4
Validation of UISSM for isotropic square plates with two opposite SS edges

Plate	Frequency parameter $\lambda = \omega a^2\sqrt{\rho/D}$					
	Mode	No. of terms taken in the infinite series (see Table 3)				Levy-type solution
		100	200	500	Infinity	
SCSS	1	23.707	23.677	23.659	23.646	23.646
	2	51.729	51.702	51.685	51.674	51.674
	3	58.851	58.748	58.687	58.646	58.646
	4	86.336	86.234	86.174	86.134	86.134
	5	100.32	100.29	100.28	100.27	100.27
SCSC	1	29.128	29.039	28.981	28.951	28.951
	2	54.892	54.817	54.772	54.743	54.743
	3	69.832	69.578	69.427	69.327	69.327
	4	95.076	94.828	94.682	94.585	94.585
	5	102.34	102.28	102.24	102.22	102.22

from the fourth significant digit—from those documented in Ref. [10]; it can be easily verified that the present results are correct. The discrepancy is probably due to the inadequate representation of the value of π in the earlier calculations, carried out, as reported in Ref. [10], in 1938.)

Some more validation studies for plates with two opposite simply supported edges are presented in Tables 5 and 6. Table 5 pertains to buckling of orthotropic plates under equal biaxial compression. Table 6 is for buckling of isotropic plates with an elastic foundation under uniaxial or equal biaxial compression, with results included for zero foundation modulus also as a special case. In both these tables, the comparison is with respect to the exact results based on conventional Levy-type equations [11,13].

Before presenting some validation studies for plates without two opposite simply supported edges, it is necessary to examine the convergence of the superposition method with reference to the number of moment coefficients considered in the series of Eq. (1) because the different edge moment coefficients are now coupled (see Eq. (16)). This convergence is as shown in Table 7 for a typical case—such rapid convergence is found for all the problems studied here and all the results tabulated here are accurate up to the last significant digit presented. It has to be pointed out that no numerical difficulties (due to overflow or underflow or ill-conditioned equations) are encountered in UISSM even when a large number of terms are considered, unlike

Table 5
Validation of UISSM for buckling of orthotropic square plates under equal biaxial compression ($N_x = N_y = -N$)

Material constants	Plate	Critical load ($a^2N/(D_{12}+2D_{66})$)	
		UISSM	Ref. [11]
$\frac{D_{11}}{(D_{12}+2D_{66})} = 4.341$	CSSS	65.9798	65.9798
	CSCS	115.2372	115.2372
$\frac{D_{22}}{(D_{12}+2D_{66})} = 1.6136$	SSFS	41. 8642	41.8643
	CSFS	67.5526	67.5527
$\mu_{21} = 5/27$			
$\frac{D_{11}}{(D_{12}+2D_{66})} = 2.432$	CSSS	38.8838	38.8851
	CSCS	66.7625	66.7658
$\frac{D_{22}}{(D_{12}+2D_{66})} = 0.2842$	SSFS	25.1914	25.1923
	CSFS	40.0076	40.0024
$\mu_{21} = 0.36$			

Table 6
Validation of UISSM for buckling of isotropic square plates resting on a foundation ($\mu = 0.3$)

Plate	$k_F a^4/D$	Critical load (a^2N/π^2D)			
		$N_x = -N,\ N_y = 0$		$N_x = -N, N_y = -N$	
		UISSM	Ref. [13]	UISSM	Ref. [13]
SSSC	0	5.740	5.740	2.663	2.663
	100	6.767	6.767	3.132	3.132
SCSC	0	7.691	7.691	3.830	3.830
	100	7.948	7.948	4.280	4.280
SSSF	0	1.402	1.402	1.055	1.055
	100	2.428	2.428	1.745	1.745
SCSF	0	1.653	1.653	1.144	1.144
	100	2.679	2.679	2.206	2.206
SFSF	0	0.952	0.952	0.932	0.932
	100	1.979	1.979	1.626	1.626

Table 7
Convergence study for free vibration of square CCSS isotropic plate

Mode	Frequency parameter ($\lambda = \omega a^2\sqrt{\rho/D}$)				
	Three terms	Five terms	Seven terms	Ten terms	Twenty terms
1	27.0500	27.0539	27.0540	27.0540	27.0540
2	60.5378	60.5385	60.5385	60.5385	60.5385
3	60.7392	60.7822	60.7855	60.7860	60.7860
4	92.7294	92.8261	92.8344	92.8360	92.8360
5	114.496	114.556	114.556	114.556	114.556

Table 8
Validation of UISSM for vibrations of a CCCC isotropic plate

Mode	Frequency parameter ($\omega a^2\sqrt{\rho/D}$)			
	$a/b = 1$		$a/b = 0.5$	
	UISSM	Ref. [14]	UISSM	Ref. [14]
1	35.9852	35.9852	24.5777	24.5777
2	73.3938	73.3938	31.8260	31.8260
3	108.2165	108.2165	44.7696	44.7696
4	131.5808	131.5808	71.0763	71.0763
5	132.2048	132.2048	87.2526	87.2526

in the conventional Levy-type methodology wherein hyperbolic functions with large arguments (directly proportional to m and n) pose problems.

Five baseline solutions are chosen for further validation studies; four of these pertain to a plate clamped all around, while the fifth is for a CFCF plate. The first is the well-known solution of Classen and Thorne [14], with results tabulated in Leissa's monograph [10], for free vibrations of an isotropic plate. This is based on a double Fourier-series representation for the deflection function along with Stokes' transformation as suggested by Green [15] to account for the fact that the zero slope conditions are violated by the assumed Fourier series and hence term-by-term differentiation is not valid. This is an analytically rigorous strong-form solution of the governing equation wherein convergence of the frequencies by appropriate truncation of the infinite characteristic determinant has been carefully ensured. The comparison of the results of UISSM with those of this baseline solution as in Table 8 shows that they agree exactly up to the last significant digit presented.

Table 9 presents the validation of UISSM for free vibration analysis of an orthotropic CCCC plate with respect to the baseline solution of Gorman [16] by the conventional superposition approach employing closed-form Levy-type solutions; a similar solution [17] for orthotropic plates with initial stresses is used in Table 10. Table 11 presents the validation study for buckling of a clamped isotropic plate with respect to the results of a multiterm extended Kantorovich solution [18], believed to be the best available so far for this particular problem. A final validation study, for the frequencies of a square isotropic CFCF plate, is presented in Table 12 with respect to the results based on Green's approach [10]. All these validation studies clearly establish the legitimacy of the untruncated series used for the individual building blocks and the accuracy of the final results based on their superposition.

Finally, for the sake of future comparisons, converged results of UISSM are tabulated for free vibrations and buckling of square orthotropic plates with different edge conditions (Tables 13 and 14), with the effect of an elastic foundation also considered for the buckling problem. The orthotropic properties correspond to a (0°) unidirectionally reinforced fibre composite with the following elastic constants:

$$E_L/E_T = 25,\ G_{LT}/E_T = 0.5,\ \mu_{LT} = 0.25,$$

Table 9
Validation of UISSM for vibrations of a CCCC orthotropic plate[a]

Mode	Frequency parameter ($\omega a^2\sqrt{\rho/D_{11}}$)			
	$a/b = 1$		$a/b = 0.5$	
	UISSM	Ref. [16]	UISSM	Ref. [16]
1	41.10	41.12	25.60	25.60
2	78.58	78.56	52.42	52.44
3	125.0	125.0	65.11	65.12
4	137.0	137.0	75.32	75.32
5	160.6	160.6	92.14	92.12

[a] $D_{12}+2D_{66} = D_{22} = 1.5D_{11}$.

Table 10
Validation of UISSM for CCCC orthotropic square plate with initial stresses ($N_x = N_y = N$)

$\frac{Na^2}{\pi^2(D_{12}+2D_{66})}$	Fundamental frequency parameter $\left(\omega a^2\sqrt{\frac{\rho}{(D_{12}+2D_{66})}}\right)$			
	Isotropic		$\frac{D_{11}}{(D_{12}+2D_{66})} = \frac{D_{22}}{(D_{12}+2D_{66})} = 2$	
	UISSM	Ref. [17]	UISSM	Ref. [17]
−2	28.573	28.573	42.641	42.641
0	35.985	35.985	47.959	47.959
10	59.925	59.925	68.165	68.165
20	76.171	76.171	83.206	83.206

Table 11
Validation of UISSM for buckling of CCCC isotropic square plate

Method	Critical load (a^2N/π^2D)	
	$N_x = -N,\ N_y = 0$	$N_x = -N,\ N_y = -N$
UISSM	10.0739	5.30362
Ref. [18]	10.0739	5.30363

Table 12
Validation of UISSM for vibrations of a square CFCF isotropic plate ($\mu = 0.3$)

Method	Frequency parameter ($\omega a^2\sqrt{\rho/D}$)				
	Mode 1	Mode 2	Mode 3	Mode 4	Mode 5
UISSM	22.17	26.40	43.60	61.20	67.20
Ref. [10]	22.17	26.40	43.60	61.20	67.20

where L and T refer to the directions parallel and transverse, respectively, to the fibres. For the sake of completeness, results of a plate simply supported all around are also included in these tables, though this case admits of a straightforward Navier-type solution. In Table 13, the nodal lines parallel to the x and y axes, respectively, corresponding to each mode shape are indicated in parentheses.

Table 13
Converged results for free vibration of orthotropic square plates

Plate	Frequency parameter $\left(\omega a^2\sqrt{\frac{\rho}{E_T h^3}}\right)$				
	Mode 1	Mode 2	Mode 3	Mode 4	Mode 5
FCFC	6.463 (0,0)	8.126 (0,1)	17.81 (1,0)	20.22 (1,1)	34.50 (0,2)
CCFC	8.745 (0,0)	19.38 (1,0)	33.56 (0,1)	36.24 (2,0)	40.00 (1,1)
SSSS	15.23 (0,0)	20.37 (1,0)	32.33 (2,0)	51.10 (3,0)	57.83 (0,1)
SCSS	15.70 (0,0)	22.36 (1,0)	36.12 (2,0)	56.55 (3,0)	58.01 (0,1)
SCSC	16.44 (0,0)	24.81 (1,0)	40.35 (2,0)	58.26 (0,1)	62.40 (3,0)
CSSS	22.98 (0,0)	26.85 (1,0)	36.98 (2,0)	54.35 (3 0)	72.87 (0,1)
SSCC	23.31 (0,0)	28.41 (1,0)	40.35 (2,0)	59.52 (3,0)	73.02 (0,1)
SCCC	23.82 (0,0)	30.39 (1,0)	44.19 (2,0)	65.11 (3,0)	73.22 (0,1)
CFCF	32.33 (0,0)	32.70 (1,0)	34.53 (2,0)	40.06 (3,0)	51.90 (4,0)
CCCF	32.46 (0,0)	33.99 (1,0)	39.29 (2,0)	51.05 (3,0)	70.22 (4,0)
CSCS	32.85 (0,0)	35.73 (1,0)	43.95 (2,0)	59.41 (3,0)	82.19 (4,0)
CSCC	33.08 (0,0)	36.92 (1,0)	46.83 (2,0)	64.18 (3,0)	88.73 (4,0)
CCCC	33.44 (0,0)	38.47 (1,0)	50.18 (2,0)	69.41 (3,0)	89.99 (0,1)

Table 14
Converged results for buckling of orthotropic square plates

Plate	Critical load $\left(\frac{a^2 N}{E_T h^3}\right)$			
	$N_x = -N,\ N_y = 0$		$N_x = N_y = -N$	
	Without foundation	% Increase due to foundation[a]	Without foundation	% Increase due to foundation[a]
FCFC	5.460	12.1	2.726	12.1
CCFC	13.63	7.8	4.399	10.0
SSSS	23.49	87.8	8.407	49.0
SCSS	24.98	82.5	9.057	39.0
SCSC	27.38	75.3	10.78	31.0
CSSS	44.90	36.7	13.64	14.9
SSCC	46.16	35.7	13.89	16.4
SCCC	48.13	34.1	15.41	19.1
CFCF	82.42	18.6	10.69	100.8
CCCF	83.12	18.4	10.75	99.7
CSCS	85.13	17.9	19.11	10.5
CSCC	86.30	17.7	19.70	9.0
CCCC	88.14	17.3	21.57	7.9

[a] $k_F = \left(\pi^4 D_{11}/a^4\right)$.

In both Tables 13 and 14, plates with different boundary conditions are listed out in the order of increasing fundamental frequency or uniaxial buckling load corresponding to compression in the x-direction; it is very interesting to see that this order is the same when these two parameters are considered. However, as can be seen from Table 13, while the fundamental frequency increases from top to bottom for the listed order of boundary conditions, the higher frequencies do not follow the same trend. Similarly, the critical load corresponding to equal biaxial compression also does not show the same trend (see Table 14) in that the CFCF and CCCF plates behave differently. This is because the biaxial critical loads for the CFCF and CCCF plates are significantly lower than their uniaxial counterparts corresponding to compression in the x-direction alone; such a significant decrease is understandable because the free edges are now subjected to compressive load and

this load is in the weaker direction of orthotropy. Another observation worth noting is that the effect of the elastic foundation on the critical load, for the chosen fixed value of the foundation parameter k_F, varies significantly depending on the edge conditions and depending on whether the plate is subjected to uniaxial or equal biaxial compression.

4. Conclusion

A new superposition approach, based on the use of Navier-type double Fourier-series solutions for the individual building blocks derived using the principle of virtual work, has been presented here. These solutions are shown to be exact counterparts of conventional Levy-type closed-form expressions and hence lead to no loss of accuracy when untruncated summation is employed. Thus, this new UISSM is as accurate and rigorous as the conventional superposition method and is much more elegant and simpler because it yields frequency and buckling equations which are of just a single compact form over the entire range; thus, the need for identifying the different possible root combinations and rewriting these equations in corresponding different forms as in the conventional superposition method is completely obviated.

It is possible to extend this method for more complicated problems involving unsymmetric laminates, off-axis layers, functionally graded materials and elastic edge supports. Some such extensions will be reported in future.

Appendix

For the first building block of Fig. 2, the deflection w is obtained as

$$w = \sum_m \sum_{n=1}^{\infty} W_{mn} \sin\left(\frac{m\pi x}{a}\right) \sin\left(\frac{n\pi y}{b}\right) e^{i\omega t} \quad \text{with} \quad W_{mn} = \frac{-2n\pi M_{bm} \cos n\pi}{b^2 \Gamma(a,b)}. \tag{A.1}$$

This series can be differentiated term by term to obtain $w_{,y}$ and $w_{,yy}$, but not the higher derivatives with respect to y. This is because the second derivative given by

$$w_{,yy} = -\sum_m \sum_{n=1}^{\infty} \left(\frac{n\pi}{b}\right)^2 W_{mn} \sin\frac{n\pi y}{b} \sin\frac{m\pi x}{a} \tag{A.2}$$

violates the non-zero moment condition at the loaded edge $y = b$; the series yields zero while the correct value is given by

$$M_y\big|_{y=b} = [-D_{12} w_{,xx} - D_{22} w_{,yy}]_{y=b} = -D_{22} w_{,yy}\big|_{y=b}$$

$$\text{i.e. } w_{,yy}\big|_{y=b} = -\sum_m \frac{M_{bm}}{D_{22}} \sin\frac{m\pi x}{a}. \tag{A.3}$$

Because of this violation of the end condition, further derivatives have to be obtained using Stokes' transformation [12]. The basic idea is to assume

$$w_{,yyy} = \sum_m \left(A_{m0} + \sum_{n=1}^{\infty} A_{mn} \cos\frac{n\pi y}{b} \right) \sin\frac{m\pi x}{a}. \tag{A.4}$$

Integration of both sides of the above equation with respect to y between the limits 0 and b yields

$$w_{,yy}\big|_0^b = \sum_m A_{m0} b \sin\frac{m\pi x}{a} \quad \text{and hence } A_{m0} = -M_{bm}/bD_{22}. \tag{A.5}$$

Similarly, multiplying both sides of Eq. (A.4) by $\cos(n\pi y/b)$ and integrating with respect to y, one gets

$$w_{,yy} \cos\frac{n\pi y}{b}\Big|_0^b + \int_0^b w_{,yy}\left(\frac{n\pi}{b}\right) \sin\frac{n\pi y}{b} dy = \sum_m A_{mn}\left(\frac{b}{2}\right) \sin\frac{m\pi x}{a}. \tag{A.6}$$

Use of Eqs. (A.2) and (A.3) in the above equation yields

$$A_{mn} = -\frac{2M_{bm}\cos n\pi}{bD_{22}} - \left(\frac{n\pi}{b}\right)^3 W_{mn} \tag{A.7}$$

and hence,

$$w_{,yyy} = \sum_m \left[-\frac{M_{bm}}{bD_{22}} - \sum_{n=1}^{\infty} \left\{ \frac{2M_{bm}\cos n\pi}{bD_{22}} + \left(\frac{n\pi}{b}\right)^3 W_{mn} \right\} \cos\frac{n\pi y}{b} \right] \sin\frac{m\pi x}{a}. \tag{A.8}$$

References

[1] D.J. Gorman, *Vibration Analysis of Plates by the Superposition Method*, World Scientific, Singapore, 1999.

[2] D.J. Gorman, W. Ding, Accurate free vibration analysis of laminated symmetric cross-ply rectangular plates by the superposition-Galerkin method, *Composite Structures* 31 (1995) 129–136.

[3] D.J. Gorman, W. Ding, The superposition-Galerkin method for free vibration analysis of rectangular plates, *Journal of Sound and Vibration* 194 (1996) 187–198.

[4] K. Bhaskar, B. Kaushik, Simple and exact series solutions for flexure of orthotropic rectangular plates with any combination of clamped and simply supported edges, *Composite Structures* 63 (2004) 63–68.

[5] K. Bhaskar, A. Sivaram, Untruncated infinite series superposition method for accurate flexural analysis of isotropic/orthotropic rectangular plates with arbitrary edge conditions, *Composite Structures* 83 (2008) 83–92.

[6] K. Bhaskar, B. Kaushik, Analysis of clamped unsymmetric cross-ply rectangular plates by superposition of simple exact double Fourier series solutions, *Composite Structures* 68 (2005) 303–307.

[7] K. Bhaskar, An elegant and rigorous analytical solution for anti-symmetric angle-ply rectangular plates with any combination of simply supported and clamped edges, *Journal of Reinforced Plastics and Composites* 25 (2006) 1679–1689.

[8] P. Umasree, K. Bhaskar, Accurate flexural analysis of clamped moderately thick cross-ply rectangular plates by superposition of exact untruncated infinite series solutions, *Journal of Reinforced Plastics and Composites* 24 (2005) 1723–1736.

[9] P. Umasree, K. Bhaskar, Analytical solutions for flexure of clamped rectangular cross-ply plates using an accurate zigzag type higher-order theory, *Composite Structures* 74 (2006) 426–439.

[10] A.W. Leissa, *Vibration of Plates*, Acoustical Society of America, Melville, USA, 1993.

[11] S.R. Soni, C.L. Amba Rao, Vibrations of orthotropic rectangular plates under inplane forces, *Computers and Structures* 4 (1974) 1105–1115.

[12] T.J. Bromwich, *An Introduction to the Theory of Infinite Series*, Macmillan, London, 1926.

[13] K.Y. Lam, C.M. Wang, X.Q. He, Canonical exact solutions for Levy-plates on two parameter foundation using Green's functions, *Engineering Structures* 22 (2000) 364–378.

[14] R.W. Claassen, C.J. Thorne, Vibrations of thin rectangular isotropic plates, *Journal of Applied Mechanics—Transactions of the ASME* 28 (1961) 304–305.

[15] A.E. Green, Double Fourier series and boundary value problems, *Proceedings of the Cambridge Philosophical Society* 40 (1944) 222–228.

[16] D.J. Gorman, Accurate free vibration analysis of clamped orthotropic plates by the method of superposition, *Journal of Sound and Vibration* 140 (1990) 391–411.

[17] S.M. Dickinson, The flexural vibration of rectangular orthotropic plates subject to inplane forces, *Journal of Applied Mechanics—Transactions of the ASME* 38 (1971) 699–700.

[18] S. Yuan, Y. Jin, Computation of elastic buckling loads of rectangular thin plates using the extended Kantorovich method, *Computers and Structures* 66 (1998) 861–867.